Energy & Environmental Science

Cite this: *Energy Environ. Sci.*, 2011, **4**, 3680

www.rsc.org/ees

PAPER

Voltage, stability and diffusion barrier differences between sodium-ion and lithium-ion intercalation materials

Shyue Ping Ong, Vincent L. Chevrier, Geoffroy Hautier, Anubhav Jain, Charles Moore, Sangtae Kim, Xiaohua Ma and Gerbrand Ceder*

Received 20th May 2011, Accepted 20th June 2011
DOI: 10.1039/c1ee01782a

To evaluate the potential of Na-ion batteries, we contrast in this work the difference between Na-ion and Li-ion based intercalation chemistries in terms of three key battery properties—voltage, phase stability and diffusion barriers. The compounds investigated comprise the layered AMO_2 and AMS_2 structures, the olivine and maricite $AMPO_4$ structures, and the NASICON $A_3V_2(PO_4)_3$ structures. The calculated Na voltages for the compounds investigated are 0.18–0.57 V lower than that of the corresponding Li voltages, in agreement with previous experimental data. We believe the observed lower voltages for Na compounds are predominantly a cathodic effect related to the much smaller energy gain from inserting Na into the host structure compared to inserting Li. We also found a relatively strong dependence of battery properties on structural features. In general, the difference between the Na and Li voltage of the same structure, ΔV_{Na-Li}, is less negative for the maricite structures preferred by Na, and more negative for the olivine structures preferred by Li. The layered compounds have the most negative ΔV_{Na-Li}. In terms of phase stability, we found that open structures, such as the layered and NASICON structures, that are better able to accommodate the larger Na^+ ion generally have both Na and Li versions of the same compound. For the close-packed $AMPO_4$ structures, our results show that Na generally prefers the maricite structure, while Li prefers the olivine structure, in agreement with previous experimental work. We also found surprising evidence that the barriers for Na^+ migration can potentially be lower than that for Li^+ migration in the layered structures. Overall, our findings indicate that Na-ion systems can be competitive with Li-ion systems.

Introduction

Rechargeable lithium-ion (Li-ion) batteries[1–4] have become a mainstay of the digital age with extensive applications in portable electronics. With Li-ion battery technology poised to move into larger scale applications such as plug-in hybrid electric vehicles (PHEVs) and electric vehicles (EVs), much research has targeted the development and optimization of lithium-ion batteries, in particular, the development of cathodes with higher energy and power densities.

The typical cathode in a Li-ion battery is an intercalation compound, which as the name implies, stores Li^+ ions by

Department of Materials Science and Engineering, Massachusetts Institute of Technology, 77 Massachusetts Ave, Cambridge, MA, 02139, USA. E-mail: gceder@mit.edu

Broader context

In recent years, there have been a resurgence in interest in sodium-ion intercalation chemistry for rechargeable battery applications. Though lithium-ion chemistry has been hugely successful and is a lynchpin of the consumer electronics age, sodium-ion chemistry can potentially be cheaper than lithium-ion chemistry and offers the exciting possibility of novel intercalation structures, some of which may not exist in their lithium equivalents. A cheaper battery would accelerate the adoption of rechargeable batteries in large-scale applications such as electric vehicles, with significant benefits to the environment. This article provides a first principles investigation of the differences between lithium-ion and sodium-ion battery chemistries in terms of three key battery properties—voltage, phase stability and diffusion barriers—over a wide range of structures commonly used in battery applications. We show that although Na voltages tend to be lower than Li voltages, this difference in voltage is highly structure dependent. We also provide surprising evidence that the barriers for Na^+ migration can potentially be lower than that for Li^+ migration in the layered structures. Overall, our findings indicate that Na-ion systems can be competitive with Li-ion systems.

inserting them into its crystal structure in a topotactic manner. Current cathodes are typically lithium transition-metal oxides or chalcogenides, which contain interstitial sites that can be occupied by Li^+. The insertion of each Li^+ is accompanied by the concomitant reduction of a transition metal ion to accommodate the compensating electron.

The earliest commercial intercalation cathode can be traced back to the work of Whittingham,[2] who first demonstrated electrochemical activity in layered $LiTiS_2$ in the 1970s. However, that material had too low a voltage to be commercially useful and was superseded by layered $LiCoO_2$ in the 1980s.[3] Although $LiCoO_2$ and its substituted variants currently dominate the world market in lithium batteries, other promising cathode materials, such as the spinel $LiMn_2O_4$[5,6] and the olivine $LiMPO_4$ materials,[4] have emerged and are increasingly finding adoption, especially in applications requiring high safety (*e.g.* PHEVs and EVs), where the thermal instability of delithiated $LiCoO_2$ proves particularly problematic.

The development of sodium batteries actually began in tandem with Li batteries in the early 1970s and 1980s.[7–12] Since then, however, research into sodium-ion (Na-ion) batteries have been sporadic,[13–15] due in no small part to the successes of Li-ion battery chemistry. Nevertheless, there has been a resurgence of research interest in Na-ion battery chemistries in recent years[16–24] because of its potential cost advantages. Sodium is far more abundant than lithium, though it has not been conclusively demonstrated that lithium reserves would be an issue in the foreseeable future. The field of sodium-ion batteries also offers the exciting possibility of novel intercalation structures, some of which may not exist in their Li equivalents.

Thus far, most research on Na-ion batteries have been experimental studies; there have been only a few computational studies, most of which are highly-targeted studies of the properties of a single compound or a few compounds.[16,25–27] First principles calculations have been used to great success in the Li-ion battery field,[28–32] and the methodologies and techniques developed in that field can similarly be applied to the Na-ion battery field.

In this work, we seek to elucidate the differences in three key battery properties—voltage, phase stability and diffusion barriers—of Na-ion and Li-ion based intercalation chemistries using first principles calculations. The compounds investigated comprise a range of known battery chemistries in a variety of different crystal structures. We attempt to correlate the observed differences between the sodium and lithium versions of these compounds with structural features.

Methods

Structure selection

In this work, we show the calculated properties of a selection of known cathode materials covering a wide range of crystal structures and transition metal chemistries for which good quality experimental data is available for comparison (with an emphasis on electrochemical data such as voltages). While we strove for an unbiased selection covering both Li-ion and Na-ion cathode compounds, our selection is no doubt skewed by the fact that Li-ion battery chemistry is far better studied than Na-ion battery chemistry, and hence, more compounds are known for Li intercalation than are known for Na intercalation. In this work, we use A to denote an alkali metal (either Li or Na) and M to denote a transition metal in generic chemical formulas representing a class of compounds.

The materials studied in this work are as follows:

1. Layered AMO_2 (M = Co, Ni, Ti) and $ATiS_2$. The traditional cathode materials are the AMO_2 layered oxides, which are favored for their high intercalation potentials and energy densities.[3] In the layered structures, the alkali A intercalates between layers of TM-centered oxygen octahedra. The $LiMO_2$ layered oxides are O3-type structures, where the oxygen planes have an ABCABC stacking sequence, while the Na equivalents typically exist in several polytypes (*e.g.* Na_xCoO_2 exists in three polytypes, O3, P2 and P3, depending on the amount of Na intercalated).[16,19,21,33–37] These polytypes differ in the stacking of the oxygen layers (ABCABC for O3, ABBA for P2 and ABBCCA for P3), resulting in different intercalation sites for the alkali cation. After complete delithiation, the MO_2 layers are weakly bound by van der Waals forces.[38] The layered oxides have been extensively studied both experimentally[5,39] and theoretically.[40–43]

Because the layered dichalcogenide, $LiTiS_2$, was once considered as a positive electrode material,[1] we have included this material in our investigations to ascertain if a different anion would modify the differences between lithium and sodium intercalation properties. Both the known Li_xTiS_2 ($P\bar{3}m1$ space group) and Na_xTiS_2 ($R\bar{3}m$ space group) structures were investigated.

2. Olivine $AMPO_4$ (M = Fe, Mn, Co, Ni). The olivine $LiMPO_4$ materials (M = Mn, Fe, Co, Ni) have emerged as a promising class of cathode materials for Li-ion batteries.[4,44–47] In particular, $LiFePO_4$ has already found widespread application in industry. Though primarily investigated for Li-ion battery cathode applications, there have been a few investigations into the Na-equivalents for potential Na-ion battery and other applications.[27,48]

The olivine structures have a *Pnma* space group and comprise vertex-sharing MO_6 octahedra, and PO_4 tetrahedra that share one edge and all vertices with MO_6 octahedra. They can be viewed as a hexagonal close-packed (hcp) array of oxygen atoms, with A or M atoms in half of the octahedral sites and P atoms in one-eighth of the tetrahedral sites. The alkali metal occupies the M(1) site (following the notation of Padhi *et al.*[4]), forming linear chains of edge-shared octahedra running parallel to the *c*-axis in the alternate *a*-*c* planes. The transition metal occupies the M(2) sites, forming zigzag planes of corner-shared octahedra running parallel to the *c*-axis in the other *a*-*c* planes.

3. Maricite $AMPO_4$ (M = Fe, Mn, Co, Ni). Maricite, as opposed to olivine, is the thermodynamically stable structure for $NaFePO_4$.[49,50] The maricite structure is similar to the olivine structure, except that the alkali occupies the M(2) site, and transition metal occupies the M(1) sites. Generally, they are of less interest for battery applications given that there are no obvious channels for fast alkali diffusion in these materials, unlike in the olivine structure.[27,51] We have included this family of compounds to study the relative stabilities of the Na and Li versions of different structures.

4. NASICON $A_3V_2(PO_4)_3$. The NASICON (Natrium Super Ionic CONductor) family of compounds have been extensively

studied as both Li-ion and Na-ion battery cathodes.[52–57] They are of the general formula $A_xMM'(XO_4)_3$ and comprise a three-dimensional framework of MO_6 and $M'O_6$ octahedra sharing corners with XO_4 tetrahedra. This framework forms large interstitial channels, which can accommodate alkali cations. In this work, we studied both the rhombohedral $R\bar{3}c$ structure preferred by $Na_3V_2(PO_4)_3$,[54] and the monoclinic $P1121/n$ structure preferred by $Li_3V_2(PO_4)_3$.[56,58]

A notable exclusion from the materials investigated is the popular spinel $LiMn_2O_4$ material.[5,6] We have excluded this material as there is no known equivalent Na spinel, and our calculations found spinel $NaMn_2O_4$ to be unstable by more than 50 meV atom^{-1} (decomposing to $NaMnO_2$, $Na_2Mn_3O_7$ and Mn_2O_3). Na^+ is apparently too large to fit in a tetrahedral site of an oxide.

As the starting point in our calculations, we used experimental structures for the alkaliated (*i.e.* lithiated or sodiated) compounds from the Inorganic Crystal Structure Database (ICSD) where available.[59] Starting structures for compounds for which there are no known experimental information (*e.g.* $NaNiPO_4$) are obtained *via* either Li-for-Na substitution or M-for-M substitution from known crystal structures. Dealkaliated (*i.e.* delithiated or desodiated) structures were obtained by removing all alkali atoms from the alkaliated structures.

Voltages

During the charging and discharging of an alkali-ion battery, an alkali A is intercalated or deintercalated from a host crystal structure A_nH. For a battery that operates by shuttling x A^+ ions between the cathode and a pure alkali metal anode, the overall cell reaction can be written as follows:

$$A_{n-x}H\ (s) + xA\ (s) \leftrightarrow A_nH\ (s)$$

where the typical phase of each compound is indicated for clarity. The forward reaction is the cell discharging reaction, while the reverse is the cell charging reaction.

The average intercalation potential V *vs.* A/A^+ can then be calculated using the following expression:[40]

$$V = -\frac{E(A_nH) - E(A_{n-x}H) - xE(A)}{xe} \quad (1)$$

where E is the total energy as calculated using DFT, and e is the absolute value of the electron charge. In this work, we calculated the average potential for a **one electron per transition metal redox reaction** for all materials, *i.e.* complete dealkaliation for the layered, maricite and olivine compounds, and removal of two alkali atoms per formula unit for the NASICON structures.

Cathodic and anodic contributions to the voltage difference between Na-ion and Li-ion battery chemistries

The overall cell reaction can be further broken down into the cathode and anode half-cell reaction as follows:

$$\text{Cathode half-cell}: \quad A_{n-x}H(s) + xA^+(solv) + xe^- \leftrightarrow A_nH(s)$$
$$\text{Anode half-cell}: \quad xA(s) \leftrightarrow xA^+(solv) + xe^-$$

where $A^+(solv)$ denotes the alkali ion solvated in the electrolyte. Only in aqueous solutions are the anodic half-cell potentials known and referenced against the standard hydrogen electrode.

The standard reduction potential for $Li^+(aq) + e^- \leftrightarrow Li(s)$ is -3.04 V. For Na, the same reaction has a standard reduction potential of -2.71 V. It is often argued that this difference of 0.33 V in the anodic half-cell potential accounts for the observed lower voltages for Na-ion batteries compared to Li-ion batteries. We believe that it is an oversimplification to attribute the difference in standard reduction potentials to the anodic contribution. Half-cell reduction potentials are dependent on the solvent and the solute concentration, *i.e.* the concentration of A^+ in the electrolyte. The standard reduction potentials for Li and Na are defined for an aqueous electrolyte with an effective concentration of 1 mol dm^{-3} of Li^+ or Na^+ ions. Another solvent would give slightly different half-cell potentials, and hence, there is no specific reason to use the aqueous potential as a standard. More importantly, the overall **thermodynamic** cell voltage is independent of the solvent, as is evident from eqn(1), and hence, the attribution of the cell voltage to cathodic and anodic contributions should similarly be independent of the solvent. In the following paragraphs, we derive a **solvent-independent** attribution of the overall cell voltage to the cathode and anode by breaking down the cathodic and anodic half-cell reactions into individual reaction steps. We argue that this leads to a more formally correct analysis of the difference between the Na and Li intercalation voltages.

For the cathode half-cell, the overall reaction can be further broken down as follows:

$$\begin{array}{ccc} A_{n-x}H\ (s) + xA^+\ (solv) + xe^- & \xrightarrow{\Delta G^{cathode}} & A_nH\ (s) \\ -x\Delta G^{A^+}_{solv}\downarrow & & \uparrow -\Delta G^{cathode}_{atom,\ A} \\ A_{n-x}H\ (s) + xA^+(g) + xe^- & \xrightarrow{-xIE} & A_{n-x}H\ (s) + xA(g) \end{array}$$

where $\Delta G^{cathode}_{atom,\ A}$ is the energy to extract an isolated atom A from the cathode, IE is the ionization energy of A, and $\Delta G^{A^+}_{solv}$ is the solvation energy of A^+.

Similarly, for the anode half-cell, the overall reaction can be broken down as follows:

$$\begin{array}{ccc} xA\ (s) & \xrightarrow{\Delta G^{anode}} & xA^+\ (solv) + xe^- \\ x\Delta G^{anode}_{atom,\ A}\downarrow & & \uparrow x\Delta G^{A^+}_{solv} \\ xA\ (g) & \xrightarrow{xIE} & xA^+\ (g) + xe^- \end{array}$$

For a pure metal anode, ΔG^{anode}_{gas} is simply the negative of the cohesive energy of the alkali metal, E^A_c.

Using the breakdown of the reaction energy contributions above, we may obtain the following expression for the voltage of the cell:

$$V = -\frac{\Delta G^{cathode} + \Delta G^{anode}}{xe} = -\frac{-x\Delta G^{A^+}_{solv} - xIE - \Delta G^{cathode}_{atom,\ A} - xE^A_c + xIE + x\Delta G^{A^+}_{solv}}{xe} \quad (2)$$

$$= \frac{\Delta G^{cathode}_{atom,\ A}}{xe} + \frac{E^A_c}{e} \quad (3)$$

From eqn (2), we may identify several possible reference states for the cathodic and anodic contributions. The traditional reference state is the alkali ion in solution A^+(solv), which implies the cathodic and anodic contributions are $\frac{x\Delta G^{A^+}_{solv} + xIE + \Delta G^{cathode}_{atom,\,A}}{xe}$ and $\frac{E^A_c - IE - \Delta G^{A^+}_{solv}}{e}$ respectively. The differences between the Na and Li cohesive energies,[60] first ionization energies[61] and hydration energies[62] are 0.530 eV, −0.253 eV, and 1.101 eV respectively. This implies that if an A^+(solv) reference is used, Na voltages should be 0.32 V lower than Li voltages, in agreement with the difference in standard reduction potentials. The most significant contribution to the difference in standard reduction potentials comes from the large 1.101 eV difference between the hydration energies of Na^+ and Li^+.

However, it is clear from eqn (3) that the ionization and solvation processes are reversed in the cathode and do not contribute to the overall voltage expression. In essence, eqn (3) is simply an explicit restatement of eqn (1) into cathodic and anodic contributions that are referenced to the atomic state of the alkali. We believe that the alkali atomic state is the relevant reference to use when comparing Li and Na voltages, given that the voltage is a thermodynamic quantity that is independent of the electrolyte.

Using the atomic reference, the cathodic contribution is $\frac{\Delta G^{cathode}_{atom,\,A}}{xe} = \frac{E(A_{n-x}H) + xE(A\ (g)) - E(A_nH)}{xe}$, and the anodic contribution is simply $\frac{E^A_c}{e}$. The conclusion from this analysis is therefore that the anodic contributions alone point to voltages for Na-ion batteries that should be 0.53 V **higher** than that for Li-ion batteries, assuming a pure metal anode.

This somewhat counter-intuitive result may be interpreted by viewing the discharge process as extracting the alkali from the metal anode (incurring the energy cost of the cohesive energy) and inserting the alkali into the host structure $A_{n-x}H$ to form A_nH (resulting in an energy gain). The smaller cohesive energy of Na implies that Na extraction from the metal anode is more facile than for Li, thereby incurring a smaller energy cost. Hence, the reason for the generally observed lower voltages for Na-ion intercalation materials relative to Li-ion intercalation materials must therefore be a cathode-related effect. We will discuss the implications of this derived result in the context of our calculated voltages in subsequent sections.

Stability

To ascertain if Na and Li prefer certain structures, we assessed the phase stabilities of all the structures studied in this work. This assessment was performed for each structure by generating the phase diagram of the corresponding system (*e.g.* Li–Co–O for $LiCoO_2$),[63,64] and determining the magnitude of the decomposition reaction energy per atom E_{decomp} to the predicted equilibrium stable phases in the phase diagram. Phases predicted to be thermodynamically stable will have $E_{decomp} = 0$, while unstable phases will have $E_{decomp} > 0$.

The phase diagrams were generated using the Materials Genome database,[65,66,93] which contains calculated energies for all unique phases in the 2006 version of the ICSD.[59] Phases not present in the ICSD but which are part of this study were manually added to the set of all ICSD phases to assess their phase stability. It should be noted that these phase diagrams are for 0 K and 0 atm, and hence, the E_{decomp} obtained from these phase diagrams are only approximate, and the actual phase stability under room temperature conditions may differ from our predictions.

Total energy calculations

All energies were calculated using the Vienna *ab initio* simulation package (VASP)[67] within the projector augmented-wave approach[68] using the Perdew–Burke–Ernzerhof generalized-gradient approximation (GGA)[69] functional and the GGA+*U* extension to it.[70] A plane wave energy cut-off of 520 eV and *k*-point density of at least 500/(number of atoms in unit cell) were used for all computations. All calculations were spin-polarized starting from a high-spin ferromagnetic configuration. For the specific compounds being investigated, we also calculated the energies of all symmetrically-distinct anti-ferromagnetic orderings for a single unit cell to determine the magnetic ground state.

The *U* values used for the various transition metals, with the exception of Co, were determined following Wang *et al.*'s approach[71] of fitting *U* so that the calculated binary oxide formation enthalpies agree with the experimental values from the Kubachewski tables.[72] For Co, the *U* value used is the average of the values determined by Zhou *et al.*[73] for delithiated and lithiated $LiCoPO_4$ olivine using a linear response scheme.[74] The reason a different *U*-fitting approach was used for Co is because the *U* value fitted using the binary Co oxide formation energies resulted in significant underestimation of voltages. The *U* values used are tabulated in Table 1.

Diffusion barriers

We investigated lithium and vacancy migration barriers in the $AFePO_4$ olivine and layered $ACoO_2$ structures using the nudged elastic band (NEB) method[75,76] as implemented in VASP.[67] In contrast to the other total energy calculations, the standard GGA functional (without the +*U* extension) was used. We chose the standard GGA functional instead of the GGA+*U* functional to avoid any mixing of the diffusion barrier with a charge transfer barrier. Given that electrons and alkali ions are likely to be strongly bound in these structures, an alkali hop in GGA+*U* is likely to be accompanied by the concomitant hopping of an electron localized on the transition metal ion nearest to the starting alkali ion site to the transition metal ion nearest to the ending alkali ion site. In some structures (*e.g.* in olivine $AFePO_4$), this electron transfer is an activated small-polaron hopping process,[77,78] and a barrier calculated with

Table 1 *U* values

Transition metal	*U*
Co	5.7 eV
Ni	6.1 eV
Fe	3.9 eV
Mn	4.0 eV
V	3.1 eV

GGA+U would be for an undefined mix of the A^+ hopping and polaron hopping processes. The same GGA functional was also used in previous works studying Li^+ diffusion in the layered and olivine structures.[43,79]

The reported alkali migration barriers were calculated using defected $1 \times 5 \times 5$ and $1 \times 2 \times 2$ supercells for the layered and olivine compounds respectively. The lattice parameters were fixed to the relaxed values of the undefected structures. For the olivine $AFePO_4$ structure in the dealkaliated limit, the defect was a single alkali inserted into a $FePO_4$ supercell. In the alkaliated limit, a single alkali vacancy was used. For the layered $ACoO_2$ structures, we investigated the barrier for migration in the alkaliated limit *via* the divacancy mechanism proposed by Van der Ven *et al.*[43] The migration pathways evaluated for the layered oxides and the olivine were the same as those used in previous studies.[43,79]

Diffusion in the maricite structure was not studied because there are no obvious diffusion channels for alkali diffusion in this structure and our preliminary investigations suggest that the alkali diffusion barrier in this structure is extremely high, making them less interesting for battery applications. The NASICON structure was also not included given the difficulties in determining diffusion pathways in the highly-open NASICON framework and the fact that Li and Na tend to occupy different sites in the NASICON.

Results

Voltages

Table 2 summarizes the calculated and experimental (where available) voltages of all the structures investigated in this work. In general, the voltages predicted by our calculations agree within 0.3 V of the experimental voltages. It should be noted that for certain structures (*e.g.* $NaCoO_2$ and $NaNiO_2$), experimental electrochemical data for a one electron per transition metal redox reaction are not available, and hence, direct comparison is not possible.

Fig. 1 shows the calculated Na voltage *versus* the Li voltage for each structure investigated. The black dashed line indicates the anodic contribution to the voltage difference between Na-ion and Li-ion battery chemistries (eqn (3)), *i.e.* the +0.53 V difference between the cohesive energies of Na and Li. Henceforth, we will denote the difference between the Na voltage and Li voltage of the same structure simply as $\Delta V_{Na-Li} = V_{Na} - V_{Li}$. This difference can be visualized as the distance of a point in the graph to the $y = x$ line. For each group of materials as indicated by the legend, a ΔV_{Na-Li} was fitted and shown as a colored line in Fig. 1. It should be noted that for all fitted lines, the slope is constrained to be 1, and that some fits were performed using only one data point. Nonetheless, the good fit obtained for the structure classes that contain at least a few compounds (*e.g.* layered, olivine and maricite) provides evidence that ΔV_{Na-Li} is structure dependent, but rather constant within a structure class. The only exception appears to be the NASICON structures, for which the rhombohedral and monoclinic structures have slightly different ΔV_{Na-Li}. It should be noted that previous work has found that Li occupies different sites from Na in the rhombohedral NASICON

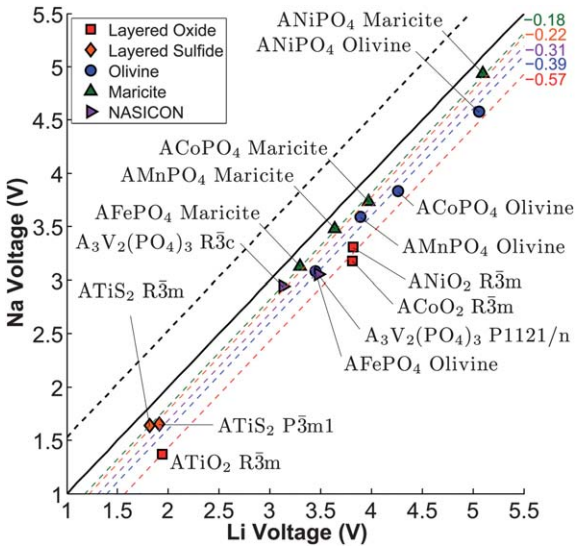

Fig. 1 Calculated Na voltage *vs.* calculated Li voltage for different structures. The black dashed line indicates the +0.53 V difference between the cohesive energies of Na and Li, while the other colored dashed lines indicate the fitted average voltage difference ΔV_{Na-Li}.

Table 2 Calculated voltages for structures investigated in this work

Formula	Structure	Space group	Source Li	Li voltage (V) Na	Na voltages (V) Calc.	Exp.	Calc.	Exp.
$ACoO_2$	Layered	$R\bar{3}m$	ICSD	ICSD	3.99	4.1[38]	3.48	> 2.8[9,36]
$ANiO_2$	Layered	$R\bar{3}m$	ICSD	ICSD	3.82	3.85[39]	3.31	> 3.0[10]
$ATiO_2$	Layered	$R\bar{3}m$	Sub.	ICSD	1.94	—	1.37	> 1.5[80]
$ATiS_2$	Layered	$P\bar{3}m1$	ICSD	Sub.	1.91	2.1[1]	1.65	—
$ATiS_2$	Layered	$R\bar{3}m$	Sub.	ICSD	1.82	—	1.64	—
$AFePO_4$	Olivine	*Pnma*	ICSD	Sub.	3.45	3.5[4]	3.08	≈ 3[27]
$AMnPO_4$	Olivine	*Pnma*	ICSD	ICSD	3.89	4.1[45]	3.59	—
$ACoPO_4$	Olivine	*Pnma*	ICSD	Sub.	4.64	4.8[46]	4.19	—
$ANiPO_4$	Olivine	*Pnma*	ICSD	Sub	5.06	5.3[47]	4.58	—
$AFePO_4$	Maricite	*Pnma*	Sub.	ICSD	3.30	—	3.13	—
$AMnPO_4$	Maricite	*Pnma*	Sub.	ICSD	3.64	—	3.48	—
$ACoPO_4$	Maricite	*Pnma*	Sub.	ICSD	4.31	—	4.09	—
$ANiPO_4$	Maricite	*Pnma*	Sub.	Sub.	5.10	—	4.94	—
$A_3V_2(PO_4)_3$	NASICON	*P*1121/*n*	ICSD	Sub.	3.48	≈ 3.6[54]	3.05	—
$A_3V_2(PO_4)_3$	NASICON	*R*3̄*c*	Ref. 54	Ref. 54	3.13	≈ 3.8[54]	2.94	—

structure,[54] but we have performed a direct substitution of Li for Na in this structure to be consistent with the other structures.

We may observe that for all structures investigated, ΔV_{Na-Li} is negative, which implies that the Na insertion into the host is significantly less favorable than Li insertion. It is well known that the $NaMPO_4$ compounds generally prefer the maricite structure over the olivine structure, while the reverse is true for $LiMPO_4$. This is borne out in our results where the ΔV_{Na-Li} for the maricite structure (−0.18 V) is significantly less negative than that for the olivine structure (−0.39 V).

For the two NASICON structures considered, the average ΔV_{Na-Li} is −0.31 V, which is in excellent agreement with the value of −0.3 V observed in a wide range of redox couples in the NASICON framework.[81] Again, we observe that the Na-preferred rhombohedral phase has a significantly less negative ΔV_{Na-Li} than the Li-preferred monoclinic phase.

The layered AMO_2 structures have the most negative ΔV_{Na-Li} of −0.57 V. We may also observe that the $ATiS_2$ structures have a much less negative ΔV_{Na-Li} than the layered oxides.

Stability

Fig. 2 shows the calculated decomposition reaction energies per atom E_{decomp} for all Na-ion and Li-ion battery compounds investigated. An E_{decomp} of zero indicates that the compound is thermodynamically stable at 0 K. In general, we found that the phase stability predicted from our calculations agree very well with the experimental literature. We may make the following observations from 2:

1. Stability of layered structures. Both the Na and Li analogues of the $ACoO_2$ and $ANiO_2$ layered structures are well known in the experimental literature. $ACoO_2$ is predicted to be stable in both the Li and Na versions in our calculations. $NaNiO_2$ is predicted to be stable as well, while the E_{decomp} of the $LiNiO_2$ structures are smaller than the accuracy limit of our DFT calculations. The experimental $R\bar{3}m$ $NaTiO_2$ phase is predicted to be stable, while the $R\bar{3}m$ $LiTiO_2$ is predicted to be unstable with respect to an ordered variant of the cubic $LiTiO_2$ (space group $Fd\bar{3}m$). For $ATiS_2$, $NaTiS_2$ is predicted to be stable in the known $R\bar{3}m$ structure, while $LiTiS_2$ is predicted to be stable in the known $P\bar{3}m1$ structure.

2. Relative stabilities of olivine and maricite structures. The known $LiFePO_4$, $LiMnPO_4$ and $LiNiPO_4$ olivines are predicted to be stable in our calculations. The known olivine $LiCoPO_4$ is not the ground state in our calculations, though its calculated E_{decomp} is reasonable at less than 10 meV $atom^{-1}$. Within the accuracy of our calculations, the maricite and olivine $NaFePO_4$ are essentially degenerate. Experiments have indicated that maricite is the thermodynamically stable form of $NaFePO_4$,[49,50] at least at the typical synthesis temperatures. Previous theoretical calculations by Moreau *et al.*[27] also found a similarly small energy difference between the two structures (though Moreau's calculations found maricite to be more stable than the olivine structure by approximately 2.3 meV $atom^{-1}$). Olivine $NaMnPO_4$ is predicted to be stable, while maricite $NaMnPO_4$ is predicted to have a small E_{decomp} of 13 meV $atom^{-1}$. Both phases are known experimentally.[82,83] Maricite $NaCoPO_4$ is predicted to be stable. Maricite $NaNiPO_4$ is predicted to have a relatively small E_{decomp} of 15 meV $atom^{-1}$, suggesting that it could potentially be metastable. All Li maricites have fairly high E_{decomp}, and it is unlikely that they would be stable.

3. Stability of NASICON structures. In agreement with previous experimental and theoretical work, the $Na_3V_2(PO_4)_3$ NASICON is predicted to be stable in the rhombohedral phase,[54] while the $Li_3V_2(PO_4)_3$ NASICON is predicted to be stable in the monoclinic phase.[56]

Diffusion barriers

Fig. 3 shows the calculated Li^+ and Na^+ migration barriers for two different intercalation structures—layered $ACoO_2$ and olivine $AFePO_4$. For layered $ACoO_2$, we calculated the barrier for a divacancy mechanism, as predicted previously by Van der Ven *et al.*[43] for a dilute vacancy $LiCoO_2$ supercell. For olivine $AFePO_4$, we calculated the barriers for a single alkali ion hop between two neighboring sites in a dealkaliated $FePO_4$ host structure as well as that for a single vacancy hop between two neighboring sites in fully alkaliated $AFePO_4$.

From Fig. 3, we may observe that the nature of the host structure has a significant impact on the relative difference between the Na and Li migration barriers. While the barriers for the divacancy diffusion in layered $ACoO_2$ are similar for both Na and Li, they are significantly different for both alkali and vacancy diffusion in the close-packed olivine structure. In fact, our calculations predict a slightly lower diffusion barrier for the divacancy mechanism in $NaCoO_2$ compared to $LiCoO_2$, which could be possibly explained by weaker Na–O bonding. For olivine $AFePO_4$, the sodium and vacancy diffusion barriers for $NaFePO_4$

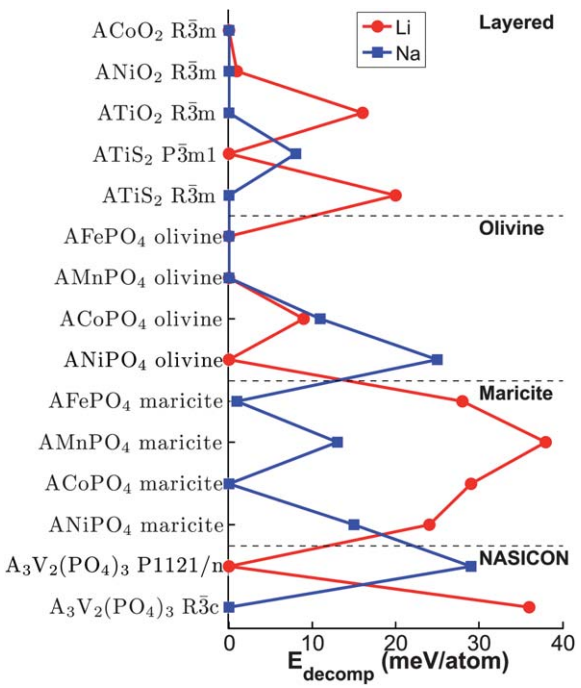

Fig. 2 Calculated decomposition reaction energies per atom, E_{decomp}, for Na-ion and Li-ion battery compounds investigated. An E_{decomp} of 0 indicates that the structure is thermodynamically stable at 0 K.

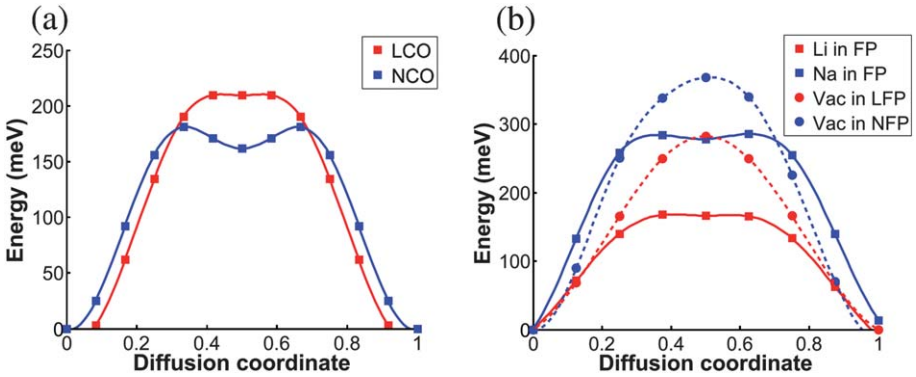

Fig. 3 Calculated diffusion barriers for two different intercalation structures.

are both predicted to be significantly higher than that of $LiFePO_4$. However, even with the highest barrier being ≈375 meV, Na-ion transport in the olivine structure should still be facile.

Discussion

In this work, we calculated the voltage, phase stability and diffusion barriers for the Na and Li analogues of a selection of intercalation compounds using first principles calculations. We found that the changes in these three properties when changing from Li-ion to Na-ion chemistry show a significant dependence on the nature of the intercalation host structures.

The insertion voltage of an alkali metal compound can be broken up into an anodic and cathodic component, each of which is referenced to the atomic state of the alkali. Such a "solvent-free" decomposition into half-cell contributions makes it clear which parts of the voltage difference between Na and Li intercalation arise from the cathode and anode specifically. The cell voltage in an alkali-ion battery is essentially given by the energy gained in inserting the alkali A into the dealkaliated host structure $A_{n-x}H$ to form A_nH, less the energy cost in extracting the alkali atom from the metal anode. Based on this analysis, the smaller cohesive energy of Na metal as compared to Li metal actually implies that the anodic contribution points to Na voltages that should be 0.53 V higher than Li voltages. The reason for the generally observed lower voltages for Na-ion *versus* Li-ion batteries must therefore be a cathodic effect, *i.e.* the energy gained from inserting Na into a host structure is much lower than that for inserting Li.

We believe that the significantly lower energy gain for Na insertion compared to Li insertion can be partially explained by the fact that Na tend to form weaker bonds with O than Li (with the exception of the $ATiS_2$ structures, the other structures are all oxides). For instance, the formation energy of Li_2O (−598.73 kJ mol^{-1}) is much greater than that of Na_2O (−417.98 kJ mol^{-1}),[84] both of which have the same crystal structure. A hypothetical Na–O battery forming Na_2O would have a voltage about 1 V lower than the equivalent Li–O battery, despite the lower cohesive energy of Na. Of course, the relative strengths of the Na–O *versus* Li–O bond would depend strongly on the local environment in the crystal. For the structures investigated in this work, the differences in voltage between the Na and Li analogues, ΔV_{Na-Li}, are far more modest, ranging from −0.18 V to −0.57 V.

Our results demonstrate that there is a relatively strong dependence of the voltage difference with crystal structure. In general, the structures that are preferred for Na will have a less negative ΔV_{Na-Li}. For example, the maricite structures preferred for many $NaMPO_4$ compounds have a ΔV_{Na-Li} that is less negative than the Li-preferred olivine structures. Similarly, the Na-preferred rhombohedral NASICON phase has a significantly less negative ΔV_{Na-Li} than the Li-preferred monoclinic phase. The layered AMO_2 structures have the most negative ΔV_{Na-Li}. We believe that this large negative ΔV_{Na-Li} for the layered structures to be the result of expansion of these structures in the *c*-direction upon alkali insertion, which accentuated the relative difference in the Na–O *versus* Li–O bond strengths. The large *c*-axis expansion upon Na insertion makes the layered structures deviate much more from close packing than is the case for $LiMO_2$ compounds. The layered $ATiS_2$ structures have less negative ΔV_{Na-Li}, and the difference in the formation enthalpies of Li_2S (−446.1 kJ mol^{-1})[72] and Na_2S (−336.1 kJ mol^{-1})[84] is also much less than the difference in the oxides (indicating that the relative difference between the Na–S and Li–S bond strengths is smaller than the relative difference between the Na–O and Li–O bond strengths).

With regards to the structural preference of Na and Li, it is evident from our results that the ability for the crystal structure to accommodate the significantly larger Na^+ ion (ionic radii of 102 pm, compared to the Li^+ ionic radii of 76 pm) is an important factor. The ability of the layered structure to accommodate different ion sizes between its layers means that stable versions of these compounds generally exist for both Na and Li. This is also true for the highly open NASICON frameworks. For the structures with close-packed oxygen frameworks, we found the decomposition energies of the Li olivines to be smaller or equal to that of the Na olivines, while the situation is reversed for the maricite structure. This is consistent with olivine (maricite) in general being the more stable structure for Li (Na) compounds. Nonetheless, most of the olivine and maricite Na compounds have relatively low decomposition energies (except olivine $NaNiPO_4$), which suggest that they could potentially be metastable. All Li maricite compounds are predicted to have very high decomposition energies, and it is unlikely that they would be stable.

The difference between the migration barriers for Na and Li motion is highly structure dependent. We found surprising evidence that Na^+ diffusion can possibly be faster than Li^+ in

certain structures. From simple intuition, one might guess that diffusion barriers of Na compounds would always be higher than that of the Li analogue due to the significantly larger ionic radius of Na^+ compared to Li^+. However, our calculations found a slightly lower barrier for the divacancy diffusion mechanism in $NaCoO_2$ compared to $LiCoO_2$. This is likely due to the larger slab spacing for layered $NaMO_2$ compounds, which has been shown to strongly influence the alkali migration barrier.[85] For olivine $AFePO_4$, our calculations predict a much higher barrier for Na diffusion compared to Li diffusion. This can be explained by the fact that the relatively rigid oxygen framework limits the ability of the structure to accommodate the larger Na^+ ion.

Implications for materials design

Our results suggest that the voltage for Na-intercalation is the key property that needs to be optimized for the development of Na-ion battery chemistry. Our calculations show that Na^+ migration barriers in the layered compounds are similar to (and may even be lower than) the corresponding Li^+ migration barriers. Though significantly higher barriers are found for Na^+ and vacancy migration in the $AFePO_4$ structure than for Li^+ migration, the barriers are still relatively low at < 375 meV.

A higher voltage can come from either a less stable dealkaliated structure, or a more stable alkaliated structure. With the exception of the NASICON structures, the desodiated and delithiated structures of the structures investigated are the same. If we adopt the premise that there is a limit to how unstable the dealkaliated structures can be before thermal stability in the charged battery becomes an issue, finding more stable sodiated structures would seem to be the preferred materials design strategy. Also, we note that there are many redox couples that have Li voltages that are beyond the 4.5 V limit of current organic electrolytes[86] (*e.g.* $LiNiPO_4$ with a predicted voltage in excess of 5 V[73]). Hence, moving to a Na-ion battery chemistry may provide the opportunity to obtain lower voltages with such compounds. However, these high-Li-voltage compounds are typically highly thermally unstable in the charged state,[87–90] and the charged Na analogues are expected to be similarly unstable.

The generally lower voltage of Na compounds also offers the potential of better intercalation anodes for Na-ion batteries than for Li-ion chemistries. For instance, despite its considerable safety advantages, spinel $Li_4Ti_5O_{12}$[91] has not found widespread adoption as an intercalation Li-ion battery anode because its voltage of 1.5 V *vs.* Li^+ is generally deemed too high, leading to a loss of energy density. For the same redox couple, we expect the Na intercalation anode to have a lower voltage, which would minimize the loss in energy density. However, Na-ion anodes designed according to current Li-ion strategies may lead to a significant decrease in volumetric energy density.[92]

We therefore are optimistic that there remains significant potential for materials design and development in Na-ion battery chemistry.

Conclusion

In this work, we studied the differences in the voltage, phase stability and diffusion barriers of Na-ion and Li-ion based intercalation chemistries using first principles calculations. The calculated Na voltages for the compounds investigated are 0.18–0.57 V lower than that of the corresponding Li voltages, in agreement with previous experimental data. We believe the lower voltage for Na compounds is predominantly a cathodic effect related to the much smaller energy gain from inserting Na into the host structure compared to inserting Li. We also found a relatively strong dependence of battery properties with structural features. In general, the difference between the Na and Li voltage of the same compound, ΔV_{Na-Li}, is less negative for the maricite structures preferred by Na, and more negative for the olivine structures preferred by Li. The layered compounds have the most negative ΔV_{Na-Li}. In terms of phase stability, we found that open structures, such as the layered and NASICON structures, that are better able to accommodate the larger Na^+ ion generally have both Na and Li versions of the same compound. For the closed-packed $AMPO_4$ structures, we found that Na generally prefers the maricite structure, while Li prefers the olivine structure, in agreement with previous experimental work. We also found surprising evidence that the barriers for Na^+ migration can potentially be lower than that for Li^+ migration in the layered structures.

Acknowledgements

This work was supported by the US Department of Energy under Contract DE-FG02−96ER45571, the BATT program under Contract DE-AC02-05CH11231 and the Office of Naval Research under Contract N00014-11-1-0212. This research was supported in part by the National Science Foundation through TeraGrid resources provided by Pittsburgh Supercomputing Center, as well as the resources provided by the National Energy Research Scientific Computing Center.

References

1 M. S. Whittingham, *Science*, 1976, **192**, 1126–7.
2 M. S. Whittingham, *J. Chem. Phys.*, 1975, **62**, 1588.
3 K. Mizushima, P. C. Jones, P. J. Wiseman and J. B. Goodenough, *Mater. Res. Bull.*, 1980, **15**, 783–789.
4 A. Padhi, K. Nanjundaswamya and J. Goodenough, *J. Electrochem. Soc.*, 1997, **144**, 1188–1194.
5 M. M. Thackeray, *J. Electrochem. Soc.*, 1995, **142**, 2558–2563.
6 M. A. Monge, J. M. Amarilla, E. Gutiérrez-Puebla, J. A. Campa and I. Rasines, *ChemPhysChem*, 2002, **3**, 367–370.
7 M. S. Whittingham, *Prog. Solid State Chem.*, 1978, **12**, 41–99.
8 A. Nagelberg and W. L. Worrell, *J. Solid State Chem.*, 1979, **29**, 345–354.
9 C. Delmas, J. Braconnier, C. Fouassier and P. Hagenmuller, *Solid State Ionics*, 1981, **3–4**, 165–169.
10 J. Braconnier, C. Delmas and P. Hagenmuller, *Mater. Res. Bull.*, 1982, **17**, 993–1000.
11 J. Molenda, C. Delmas and P. Hagenmuller, *Solid State Ionics*, 1983, **9–10**, 431–435.
12 J. M. Tarascon and G. W. Hull, *Solid State Ionics*, 1986, **22**, 85–96.
13 C. Delmas, F. Cherkaoui, A. Nadiri and P. Hagenmuller, *Mater. Res. Bull.*, 1987, **22**, 631–639.
14 M. Doeff, S. J. Vrsco, Y. Ma, M. Peng, L. Ding and L. C. De Jonghe, *Electrochim. Acta*, 1995, **40**, 2205–2210.
15 J. Morales, J. Santos and J. L. Tirado, *Solid State Ionics*, 1996, **83**, 57–64.
16 G. Shu and F. Chou, *Phys. Rev. B: Condens. Matter Mater. Phys.*, 2008, **78**, 3–6.
17 F. Sauvage, L. Laffont, J.-M. Tarascon and E. Baudrin, *Inorg. Chem.*, 2007, **46**, 3289–94.
18 H. Zhuo, X. Wang, A. Tang, Z. Liu, S. Gambo and P. Sebastian, *J. Power Sources*, 2006, **160**, 698–703.

19 H. Zandbergen, M. Foo, Q. Xu, V. Kumar and R. Cava, *Phys. Rev. B: Condens. Matter Mater. Phys.*, 2004, **70**, 1–8.
20 S. Komaba, T. Mikumo, N. Yabuuchi, A. Ogata, H. Yoshida and Y. Yamada, *J. Electrochem. Soc.*, 2010, **157**, A60.
21 S. Komaba, C. Takei, T. Nakayama, A. Ogata and N. Yabuuchi, *Electrochem. Commun.*, 2010, **12**, 355–358.
22 J. Whitacre, A. Tevar and S. Sharma, *Electrochem. Commun.*, 2010, **12**, 463–466.
23 L. S. Plashnitsa, E. Kobayashi, Y. Noguchi, S. Okada and J.-i. Yamaki, *J. Electrochem. Soc.*, 2010, **157**, A536.
24 J. Zhao, J. He, X. Ding, J. Zhou, Y. Ma, S. Wu and R. Huang, *J. Power Sources*, 2010, **195**, 6854–6859.
25 K. Sánchez, P. Palacios and P. Wahnón, *Phys. Rev. B*, 2008, **78**, 1–6.
26 Y. Hinuma, Y. Meng and G. Ceder, *Phys. Rev. B: Condens. Matter Mater. Phys.*, 2008, **77**, 1–16.
27 P. Moreau, D. Guyomard, J. Gaubicher and F. Boucher, *Chem. Mater.*, 2010, **22**, 4126–4128.
28 G. Ceder, M. Aydinol and A. Kohan, *Comput. Mater. Sci.*, 1997, **8**, 161–169.
29 G. Ceder, Y.-M. Chiang, D. Sadoway, M. Aydinol, Y.-I. Jang and B. Huang, *Nature*, 1998, **392**, 694–696.
30 Y. S. Meng and M. E. Arroyo-de Dompablo, *Energy Environ. Sci.*, 2009, **2**, 589–609.
31 G. Ceder, *MRS Bull.*, 2010, **35**, 693–702.
32 G. Ceder, G. Hautier, A. Jain and S. P. Ong, *MRS Bull.*, 2011, **36**, 185–191.
33 C. Delmas, C. Fouassier and P. Hagenmuller, *Physica B+C*, 1980, **99**, 81–85.
34 Y. Takeda, K. Nakahara, M. Nishijima, N. Imanishi, O. Yamamoto, M. Takano and R. Kanno, *Mater. Res. Bull.*, 1994, **29**, 659–666.
35 R. J. Balsys and R. L. Davisb, *Solid State Ionics*, 1996, **93**, 279–282.
36 R. Berthelot, D. Carlier and C. Delmas, *Nat. Mater.*, 2010, **10**, 74–80.
37 C. Didier, M. Guignard, C. Denage, O. Szajwaj, S. Ito, I. Saadoune, J. Darriet and C. Delmas, *Electrochem. Solid-State Lett.*, 2011, **14**, A75–A78.
38 G. G. Amatucci, J. M. Tarascon and L. C. Klein, *J. Electrochem. Soc.*, 1996, **143**, 1114–1123.
39 C. Delmas, M. Menetrier, L. Croguennec, S. Levasseur, J. Peres, C. Pouillerie, G. Prado, L. Fournes and F. Weill, *Int. J. Inorg. Mater.*, 1999, **1**, 11–19.
40 M. K. Aydinol, A. F. Kohan, G. Ceder, K. Cho and J. Joannopoulos, *Phys. Rev. B: Condens. Matter*, 1997, **56**, 1354–1365.
41 C. Wolverton and A. Zunger, *J. Electrochem. Soc.*, 1998, **145**, 2424–2431.
42 G. Ceder, J. Reed and A. Van Der Ven, *Electrochem. Solid-State Lett.*, 2001, **4**, A78.
43 A. Van Der Ven and G. Ceder, *Electrochem. Solid-State Lett.*, 2000, **3**, 301–304.
44 A. Yamada, S. Chung and K. Hinokuma, *J. Electrochem. Soc.*, 2001, **148**, A224–229.
45 G. Li, H. Azuma and M. Tohda, *Electrochem. Solid-State Lett.*, 2002, **5**, A135.
46 K. Amine, H. Yasuda and M. Yamachi, *In Situ*, 2000, **3**, 178–179.
47 J. Wolfenstine and J. Allen, *J. Power Sources*, 2005, **142**, 389–390.
48 N. Le Poul, E. Baudrin, M. Morcrette, S. Gwizdala, C. Masquelier and J.-M. Tarascon, *Solid State Ionics*, 2003, **159**, 149–158.
49 J. N. Bridson, S. E. Quinlan and P. R. Tremaine, *Chem. Mater.*, 1998, **10**, 763–768.
50 P. Tremaine, *J. Chem. Thermodyn.*, 1999, **31**, 1307–1320.
51 B. L. Ellis, W. R. M. Makahnouk, Y. Makimura, K. Toghill and L. F. Nazar, *Nat. Mater.*, 2007, **6**, 749–53.
52 J. Goodenough, H. Hong and J. Kafalas, *Mater. Res. Bull.*, 1976, **11**, 203–220.
53 C. Delmas, A. Nadiri and J. Soubeyroux, *Solid State Ionics*, 1988, **28–30**, 419–423.
54 J. Gaubicher, C. Wurm, G. Goward, C. Masquelier and L. Nazar, *Chem. Mater.*, 2000, **12**, 3240–3242.
55 S. Patoux and C. Masquelier, *Chem. Mater.*, 2002, **14**, 5057–5068.
56 D. Morgan, G. Ceder, J. Barker, M. Saidi, J. Swoyer, H. Huang and G. Adamson, *Chem. Mater.*, 2002, **14**, 4684–4693.
57 S. Patoux, G. Rousse, J.-B. Leriche and C. Masquelier, *Chem. Mater.*, 2003, **15**, 2084–2093.
58 M. Y. Saıdi, J. Barker, H. Huang, J. L. Swoyer and G. Adamson, *Electrochem. Solid-State Lett.*, 2002, **5**, A149.
59 G. Bergerhoff, R. Hundt, R. Sievers and I. D. Brown, *Journal of chemical information and computer sciences*, 1983, **23**, 66–69.
60 R. T. Poole, *Am. J. Phys.*, 1980, **48**, 536.
61 *CRC Handbook of Chemistry and Physics, Internet Version 2011*, ed. D. R. Lide, 91st ed.; CRC Press, 2010; pp 10–203–10–205.
62 Y. Marcus, *Ion Solvation*; John Wiley & Sons, 1985; p 306.
63 L. Wang, T. Maxisch and G. Ceder, *Chem. Mater.*, 2007, **19**, 543–552.
64 S. P. Ong, L. Wang, B. Kang and G. Ceder, *Chem. Mater.*, 2008, **20**, 1798–1807.
65 A. Jain, G. Hautier, C. J. Moore, S. Ping Ong, C. C. Fischer, T. Mueller, K. A. Persson and G. Ceder, *Comput. Mater. Sci.*, 2011, **50**, 2295–2310.
66 A. Jain; S. P. Ong; G. Hautier; G. Ceder, *Materials Genome*, 2010; http://materialsgenome.org/.
67 G. Kresse and J. Furthmuller, *Phys. Rev. B: Condens. Matter*, 1996, **54**, 11169–11186.
68 P. E. Blochl, *Phys. Rev. B: Condens. Matter*, 1994, **50**, 17953–17979.
69 J. P. Perdew, M. Ernzerhof and K. Burke, *J. Chem. Phys.*, 1996, **105**, 9982.
70 V. I. Anisimov, F. Aryasetiawan and A. I. Lichtenstein, *J. Phys.: Condens. Matter*, 1997, **9**, 767–808.
71 L. Wang, T. Maxisch and G. Ceder, *Phys. Rev. B: Condens. Matter Mater. Phys.*, 2006, **73**, 195107.
72 O. Kubaschewski; C. B. Alcock; P. J. Spencer, *Materials Thermochemistry*, sixth ed.; Butterworth-Heinemann, 1993; Chapter 5, p 376.
73 F. Zhou, M. Cococcioni, C. A. Marianetti, G. Ceder and D. Morgan, *Phys. Rev. B: Condens. Matter Mater. Phys.*, 2004, **70**, 235121.
74 M. Cococcioni and S. de Gironcoli, *Phys. Rev. B: Condens. Matter Mater. Phys.*, 2005, **71**, 035105.
75 H. Jonsson; G. Mills; K. W. Jacobsen, *Classical and Quantum Dynamics in Condensed Phase Simulations - Proceedings of the International School of Physics*; World Scientific Publishing Co. Pte. Ltd.: Singapore, 1998; pp 385–404.
76 G. Mills and H. Jónsson, *Phys. Rev. Lett.*, 1994, **72**, 1124–1127.
77 T. Maxisch, F. Zhou and G. Ceder, *Phys. Rev. B: Condens. Matter Mater. Phys.*, 2006, **73**, 104301.
78 S. P. Ong, V. Chevrier and G. Ceder, *Phys. Rev. B: Condens. Matter Mater. Phys.*, 2011, **83**, 075112.
79 D. Morgan, A. Van Der Ven and G. Ceder, *Electrochem. Solid-State Lett.*, 2004, **7**, A30.
80 A. Maazaz, C. Delmas and P. Hagenmuller, *J. Inclusion Phenom.*, 1983, **1**, 45–51.
81 C. Masquelier; S. Patoux; C. Wurm; M. Morcrette, in *Lithium Batteries: Science and Technology*; ed. G.-A. Nazri, G. Pistoia; Springer, 2003; Chapter 15, p 728.
82 P. B. Moore, *AMERICAN MINERALOGIST*, 1972, **57**, 1333.
83 J. Moring and E. Kostiner, *J. Solid State Chem.*, 1986, **61**, 379–383.
84 M. W. Chase, *NIST-JANAF Thermochemical Tables*, Vol. 12; American Chemical Society: New York, 1998.
85 K. Kang and G. Ceder, *Physical Review B*, 2006, **74**, 1–7.
86 K. Xu, *Chem. Rev.*, 2004, **104**, 4303–4418.
87 N. N. Bramnik, K. Nikolowski, D. M. Trots and H. Ehrenberg, *Electrochem. Solid-State Lett.*, 2008, **11**, A89.
88 G. Chen and T. J. Richardson, *J. Power Sources*, 2010, **195**, 1221–1224.
89 S.-W. Kim, J. Kim, H. Gwon and K. Kang, *J. Electrochem. Soc.*, 2009, **156**, A635.
90 S. P. Ong, A. Jain, G. Hautier, B. Kang and G. Ceder, *Electrochem. Commun.*, 2010, **12**, 427–430.
91 E. Ferg, R. J. Gummow, A. de Kock and M. M. Thackeray, *J. Electrochem. Soc.*, 1994, **141**, L147.
92 V. L. Chevrier and G. Ceder, *J. Electrochem. Soc.*, 2011, **158**(9), A1011.
93 A. Jain, G. Hautier, S. Ong, C. Moore, C. Fischer, K. Persson and G. Ceder, *Phys. Rev. B*, 2011, **84**(4), 045115.

